# Catalytic properties of silica supported titanium, vanadium and niobium oxide nanoparticles towards the oxidation of saturated and unsaturated hydrocarbons

Susana Martínez-Méndez [1], Yurgenis Henríquez, Olgioly Domínguez [2], Lindora D'Ornelas *, Heinz Krentzien

*Laboratorio de Síntesis Organometálica, Centro de Química Organometálica y Macromolecular, Escuela de Química, Facultad de Ciencias, Universidad Central de Venezuela, Av. Los Ilustres, Los Chaguaramos, Apdo Postal 47778, Caracas 1040, Venezuela*

## Abstract

The catalytic properties of silica supported titanium, vanadium and niobium oxide nanoparticles towards the oxidation of different organic substrates (cyclohexane, cyclohexene, 1-hexene) using tertbutylhydroperoxide (TBHP) and molecular oxygen as the oxidizing agents was studied. Titanium (1.9 nm), vanadium (2.3 nm) and niobium (1.6 nm) oxide nanoparticles stabilized on silica were synthesized by the reduction of $TiCl_4 \cdot 2THF$, $VCl_3 \cdot 3THF$ and $NbCl_4 \cdot 2THF$ with $K[BEt_3H]$. These materials were characterized by inductive coupled plasma-optical emission spectroscopy (ICP-OES), Fourier transformed infrared spectroscopy (FTIR), high resolution transmission electron microscopy (HRTEM) and X-ray photoelectron spectroscopy (XPS) analyses. The solids obtained were employed as heterogeneous catalysts. For 1-hexene and cyclohexene, the titanium oxide nanostructured material showed 100% selectivity towards the epoxidation product, with conversions above 50%. In the case of cyclohexane, the titanium oxide nanoparticles are 100% selective towards the desired oxidation products (cyclohexanol and cyclohexanone). The highest oxidation activity was achieved with the vanadium oxide nanoparticles for the three substrates studied: cyclohexane, cyclohexene and 1-hexene, TN 562, 878 and 1190 mol of product/mol of metal, respectively, after 6 h of reaction time at 80 °C. Nevertheless, with this metal the selectivity is different to the one obtained for with the titanium oxide nanostructured system. The niobium catalyst was less active than the titanium and vanadium oxide catalysts, although it proved to be more selective towards the formation of alcohols.
© 2006 Elsevier B.V. All rights reserved.

*Keywords:* Nanoparticles; Oxidation catalysts; Vanadium; Niobium; Titanium; Epoxidation

## 1. Introduction

The oxidation of organic substrates represents one of the most important industrial chemical reactions [1], explaining the significant effort invested in the research and development of new heterogeneous catalysts with increased activities and selectivities in these types of reactions. In particular, alkene epoxidation is one of the main aims in this area [2,3]. The oxidation of cyclohexane and cyclohexene to cyclohexanol and cyclohexanone is the key reaction in the synthesis of adipic acid, which is an essential precursor in the production of nylon 6 and nylon 66 [4].

It is well known that amongst the most active homogeneous and heterogeneous catalysts for alkene and alkane oxidation, are those based on transition metals of groups 4 (Ti), 5 (V and Nb) and 6 (Mo) [5–10]. In the case of heterogeneous catalysts, it has been proved that a proper selection of preparation conditions is essential to obtain a homogeneous metal dispersion on the support, which in turn, generates highly active and selective catalysts towards oxidation reactions [9–14].

Over the last decade, the research and development of transition metal nanoparticles has received a lot of attention in many

---

* Corresponding author. Tel.: +58 212 605 1343; fax: +58 212 605 1256.
  *E-mail address:* ldornela@strix.ciens.ucv.ve (L. D'Ornelas).
[1] Permanent address: PDVSA-INTEVEP, Apartado 76343, Caracas 1070, Venezuela.
[2] Permanent address: Departamento the Quimica Aplicada, Fac. de Ingeniería, Universidad Central de Venezuela, Av. Los Ilustres, Los Chaguaramos, Caracas 1040, Venezuela.

areas of science. This interest is because nanosized particles show different physical and chemical properties to those of the same materials in the bulk [15,16]. The main reasons for these differences originate in the electronic properties and in the very high ratio between superficial atoms and total number of atoms in the particles found in these nanomaterials. Both properties mentioned above, are of interest from the catalytical point of view, since they can aid in raising the activity and selectivity of a reaction and, in some cases, induce new reactivities and selectivities never observed with classical catalysts [15–17].

This work presents a catalytic study of the oxidation of saturated and unsaturated hydrocarbons with titanium, vanadium and niobium oxide nanoparticle systems supported on silica.

## 2. Experimental

### 2.1. Materials

All the syntheses were carried out under an argon atmosphere (99.99% pure) using Schlenk techniques for the manipulation of air sensitive compounds [18].

The metal precursors $TiCl_4 \cdot 2THF$ (Aldrich), $VCl_3 \cdot 3THF$ (Strem) $NbCl_4 \cdot 2THF$ (Strem) were used as supplied.

The silica gel (Gomasil G-200) used as inorganic support is 98.8% $SiO_2$ and 0.69% $Na_2SO_4$ content, with a mean grain size of 0.5 μm. The silica gel was activated at 250 °C under vacuum during 72 h, and then kept under an argon atmosphere before its use. After activation, the $SiO_2$ showed a BET specific surface area of 169 $m^2/g$. Rhodia Silices de Venezuela C.A. donated this material.

### 2.2. Synthesis of the silica supported metal oxide nanoparticles

To obtain the metal oxide nanoparticles supported on silica, firstly the metallic nanoparticles of titanium, vanadium and niobium were synthesized following the method established by Bönnemann [19], then stabilized on silica and finally oxidized under 1 atm of molecular oxygen.

As an example, here follows the procedure for the synthesis of niobium oxide nanoparticles. A solution of $K[BEt_3H]$ (1 M, 80 ml, 80 mmol) in tetrahydrofurane (THF) was added dropwise to a suspension of $NbCl_4 \cdot 2THF$ (10.24 g, 20 mmol) in THF at room temperature during 2 h. After 2 h of constant stirring at room temperature, a dark brown solution was obtained. The KCl formed during the reaction was removed by filtration and the solvent was eliminated under vacuum. A dark solid was obtained which later was redissolved in fresh THF and added to a silica/THF suspension. This suspension was stirred for at least 8 h, and then dried under vacuum during 24 h resulting in a light brown solid. All three silica supported nanoparticles (titanium, vanadium and niobium) are extremely sensitive to air.

Finally, the nanometric metal oxides supported on silica are obtained by the exposure of the previously synthesized systems to 1 atm of molecular oxygen.

### 2.3. Characterization of the silica supported metal oxide nanoparticles

Routine FTIR was performed on a Perkin-Elmer 1760-X spectrometer using CsI disks. The elemental analyses were carried out by atomic emission with coupled inductive plasma on a Thermo Jarrel ASH model IRIS H12. The high resolution transmission electron microscopy (HRTEM) was carried out in a CM30 Phillips Microscope with a 0.19 nm resolution. Samples were prepared using carbon-coated copper grids. One drop of a THF suspension of $[M_xO_y/SiO_2]$ was placed on the carbon-coated grid using a microsyringe. Different samples of each nanostructured materials were prepared; these samples were subject to scanning in entire the area verifying the homogeneity of the nanoparticles dispersion. The size and size distribution of the nanoparticles was determined through manual analysis enhancing the contrast of the digital micrographs, which are the output of the HRTEM, at least 100 particles per sample were measured. This analysis was corroborated employing Image Pro Plus 5.0 as a digital processing program.

The X-ray photoelectron spectroscopy, XPS, was carried out in a Escalab 220i-XL equipped with a monochromatic source Mg Kα ($h\gamma = 1253.6$ eV). The deconvolutions of the XPS spectra were carried out using a XPS Peak Fitting program version 4.1.

Gas chromatography (GC) analyses were performed on a Perkin-Elmer Autosystem XL with a flame ionization detector (FID), equipped with a PE-Alumina capillary column (30 m). Gas chromatography coupled with mass spectroscopy (GC–MS) was performed on a HP6890 equipped with a Mass Selective Detector 5973.

### 2.4. Catalytic activity

The catalytic studies of the solids obtained, were carried out in Fischer–Porter bottles. Metal supported catalyst (100 mg) was introduced in the Fischer–Porter bottle along with 2 ml of organic substrate (cyclohexane, cyclohexene and 1-hexene) and 0.5 ml of TBHP as the oxidizing agent. The reactions were carried out under 1 atm of argon or 3 atm of molecular oxygen and at 80 °C. This study was done in order to determine the influence of molecular oxygen in the catalytic activity of the solid towards oxidation reaction. All reactions were studied with different reaction times.
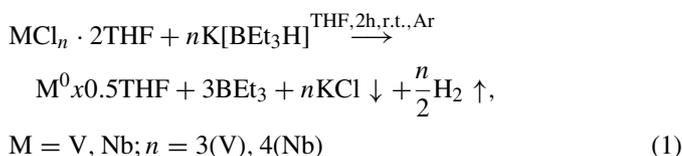
The TBHP percentage was determined through iodometric analysis, before and after catalytic oxidation reaction [20].

## 3. Results and discussions

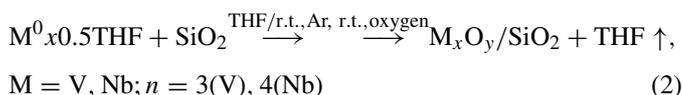### 3.1. Synthesis and characterization of nanostructured systems

The titanium, vanadium and niobium oxide nanoparticles were synthesized firstly following the method established by Bönnemann [19] for the preparation of metallic nanoparticles, then stabilized on silica and finally oxidized under 1 atm of molecular oxygen.

The Bönnemann method [19] employs the reduction of the metal adduct $TiCl_4 \cdot 2THF$, $VCl_3 \cdot 3THF$ and $NbCl_4 \cdot 2THF$ with $K[BEt_3H]$ at room temperature and under an argon atmosphere. As described by this author, highly pyrophoric black powders are obtained from these syntheses. At this stage, he reports that the black solids obtained are metallic nanoparticles stabilized with THF as suggested in Eq. (1):

$$MCl_n \cdot 2THF + nK[BEt_3H] \xrightarrow{THF, 2h, r.t., Ar}$$
$$M^0 x 0.5THF + 3BEt_3 + nKCl \downarrow + \frac{n}{2}H_2 \uparrow,$$
$$M = V, Nb; n = 3(V), 4(Nb) \tag{1}$$

Due to the high reactivity of the THF stabilized metallic nanoparticles of titanium, vanadium and niobium with air, the XPS analyses only showed the presence of the oxidized species. As an example, Fig. 1 shows the XPS spectrum for the titanium nanometric system stabilized with THF, where two different signals in the Ti $2p_{3/2}$ region with binding energies at 457.9 and 458.3 eV characteristic of $TiO_2$ [21,22], can be seen.

Once the metallic nanoparticles stabilized with THF are obtained, they are supported on silica under an argon atmosphere (Eq. (2)). The solids obtained are light grey in the case of the titanium system and brown in the case of the vanadium and niobium systems. When these systems were exposed to molecular oxygen (1 atm), they all immediately turn into white powders.

$$M^0 x 0.5THF + SiO_2 \xrightarrow{THF/r.t., Ar, \ r.t., oxygen} M_xO_y/SiO_2 + THF \uparrow,$$
$$M = V, Nb; n = 3(V), 4(Nb) \tag{2}$$

The solids exposed to molecular oxygen were characterized via ICP-OES, XPS and HRTEM.

The characterization via ICP-OES of $TiO_2/SiO_2$, $V_2O_5/SiO_2$ and $Nb_2O_5/SiO_2$ show metal contents for titanium, vanadium and niobium of 1.8%, 0.62% and 0.92% in weight, respectively.

The XPS spectrum for the titanium/silica system exposed to molecular oxygen (Fig. 2) shows three different signals in the Ti $2p_{3/2}$ region with binding energies at 458.3, 459.3 and 461.1 eV, all of which are characteristic of $TiO_2$ species in different environments [21,22].
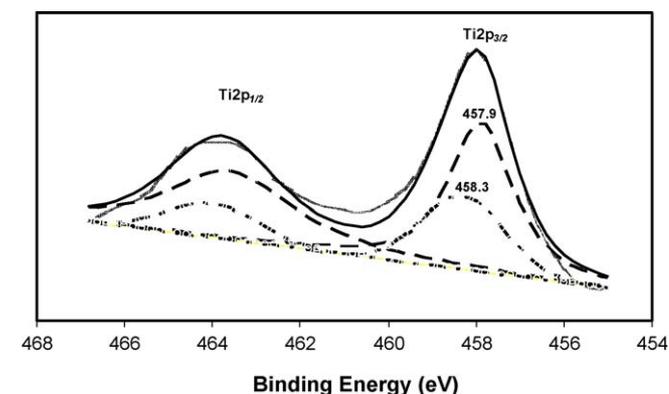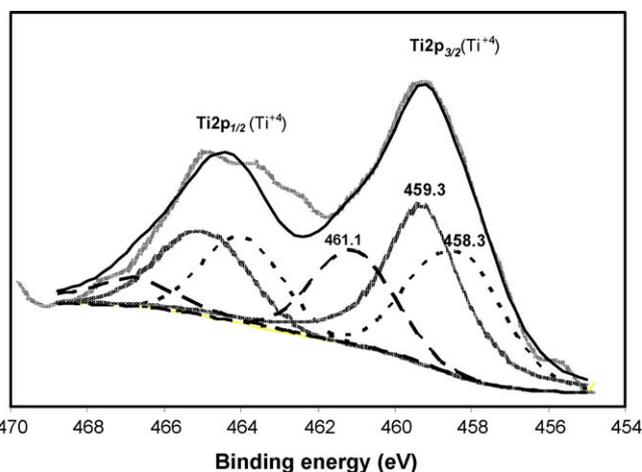


Fig. 2. The Ti $2p_{3/2}$ and Ti $2p_{1/2}$ XPS spectra for the titanium/silica nanostructured system exposed to molecular oxygen (1 atm).

For the niobium/silica system exposed to molecular oxygen (1 atm), the XPS spectrum deconvolution (Fig. 3) displays signals in the region for Nb $3d_{5/2}$ characteristic of niobium species in different oxidation states: at 204.4 eV ($Nb^{2+}$), 205.5 eV ($Nb^{4+}$) and 207.0 eV ($Nb^{5+}$) [21,23]. It is evident from the deconvolution that the most oxidized species ($Nb_2O_5$) has the predominant contribution.

For the vanadium/silica systems exposed to molecular oxygen (1 atm), due to the low vanadium concentration, the XPS spectrum shows a very small signal at 516.5 eV in the region for V $2p_{3/2}$ characteristic of $V_2O_5$; this signal is overlapped by the O 1s X-ray satellite of the silica, which makes its deconvolution impossible. This spectrum is not shown here.

The HRTEM analysis (micrographs and histograms) for the $TiO_2/SiO_2$, $V_2O_5/SiO_2$ and $Nb_2O_5/SiO_2$ systems are shown in Figs. 4–6, respectively. Due to the silica support, the contrast of these materials is rather poor and the best contrast area was



Fig. 1. The Ti $2p_{3/2}$ and Ti $2p_{1/2}$ XPS spectra for the titanium nanostructured system stabilized with THF.
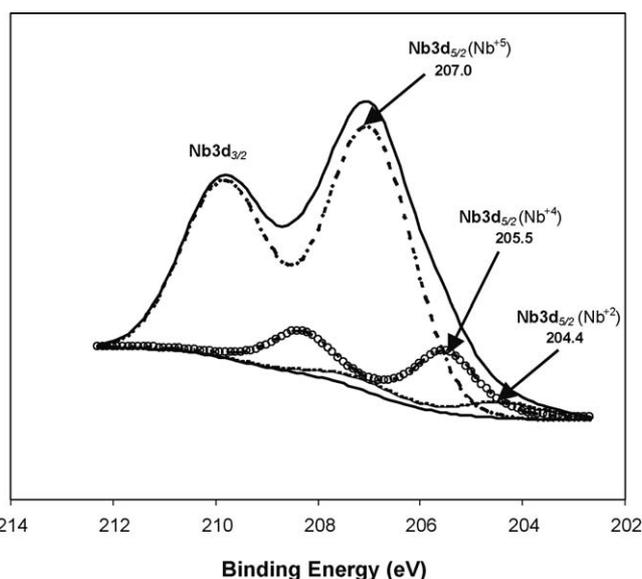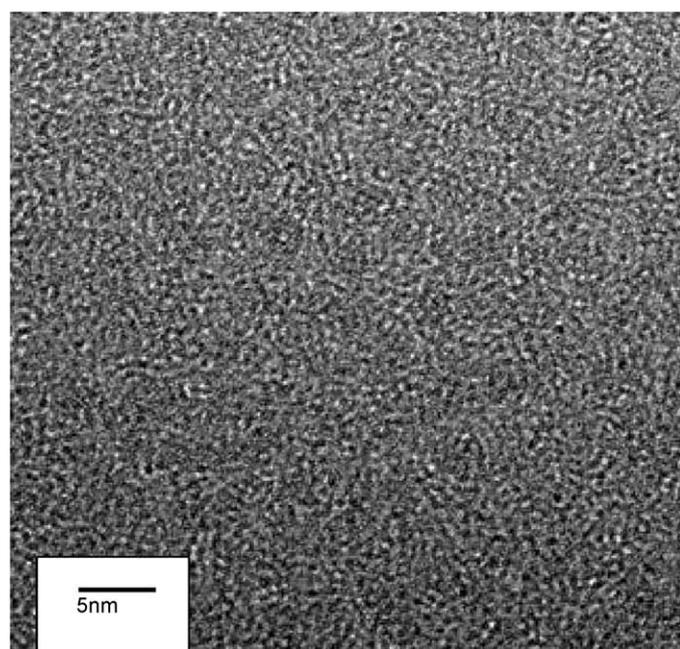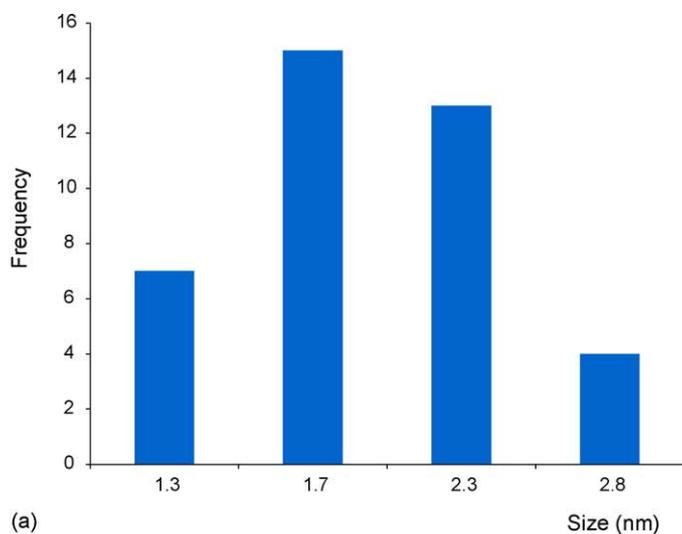


Fig. 3. The Nb $3d_{5/2}$ and Nb $3d_{3/2}$ XPS spectra for the niobium/silica nanostructured system exposed to molecular oxygen (1 atm).
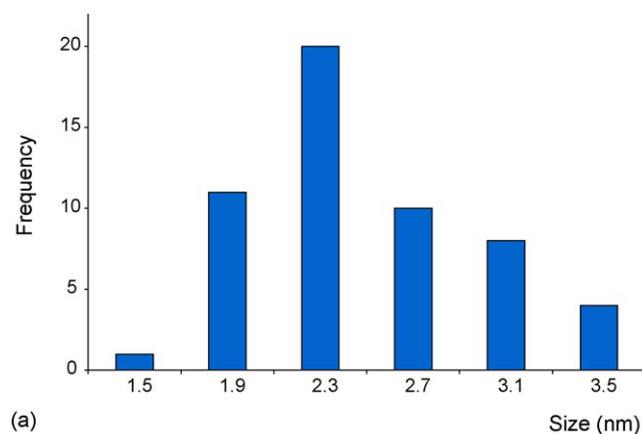
(a)



(b)

Fig. 4. Micrography and histogram for silica supported titanium oxide nanoparticles, TiO$_2$/SiO$_2$, obtained from the reduction of TiCl$_4$·2THF with K[BEt$_3$H].



(a)



(b)

Fig. 5. Micrography and histogram for silica supported vanadium oxide nanoparticles, V$_2$O$_5$/SiO$_2$, obtained from the reduction of VCl$_3$·3THF with K[BEt$_3$H].
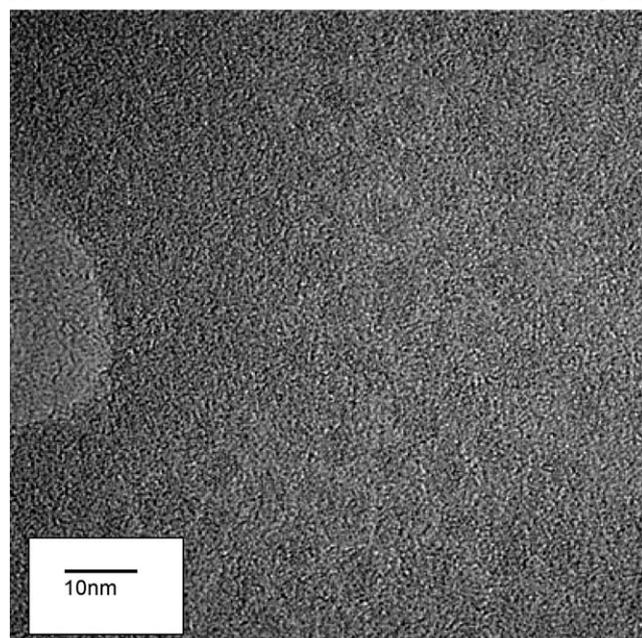
selected for the respective micrographs. All of these materials show a homogeneous dispersion on the support and have spherical morphology. The titanium system shows nanoparticle sizes ranging from 1.2 to 2.9 nm and a mean size of 1.9 nm (Fig. 4). In the vanadium system the size distribution, ranges between 1.5 and 3.5 nm, with a mean particle size of 2.5 nm (Fig. 5). For the niobium system the particle size distribution ranges from 0.8 to 2.2 nm; the mean size for these particles is 1.6 nm (Fig. 6).

## 3.2. Catalytic reactivities of nanostructured systems

The catalytic studies were carried out with the oxidized solid systems TiO$_2$/SiO$_2$, V$_2$O$_5$/SiO$_2$ and Nb$_2$O$_5$/SiO$_2$, in a Fischer–Porter bottle at 80 °C using TBHP as the limiting oxi-dizing agent, in the presence of molecular oxygen (3 atm) or argon (1 atm), using 1-hexene, cyclohexene and cyclohexane as substrates. No solvent was introduced in the reaction mixture. It is worth noting that the TiO$_2$/SiO$_2$ catalyst turns yellow in the presence of TBHP or H$_2$O$_2$. This colour change is attributed to the formation of Ti–OOR species [24,25].

Table 1 details the catalytic activities of the silica supported titanium oxide nanoparticles towards the oxidation of the different studied substrates. In the presence of molecular oxygen for the [TiO$_2$/SiO$_2$] system, turnover numbers (TN = mol of product/mol of metal) of 321.6, 309.0 and 133.0 for 1-hexene, cyclohexene and cyclohexane, respectively, were obtained after 6 h of catalytic oxidation. These represent 77.5% conversion of 1-hexene, 68.4% conversion of cyclohexene and 19.2% conversion of cyclohexane. The selectivity was 100% towards the epoxide for 1-hexene and cyclohexene, whereas with the cyclohexane 100% selectivity towards the formation of cyclohexanol (58%) and cyclohexanone (42%) was found. Fig. 7 shows the

(a)
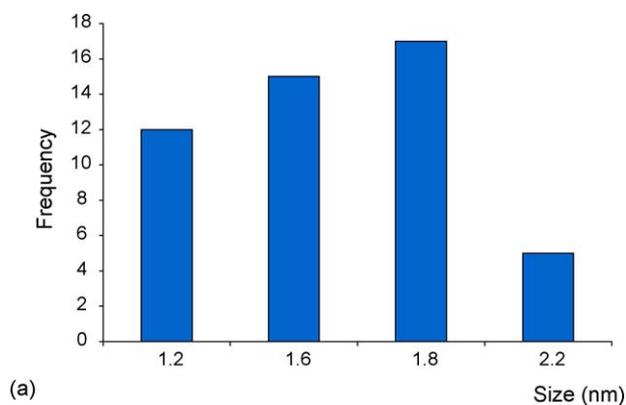


(b)
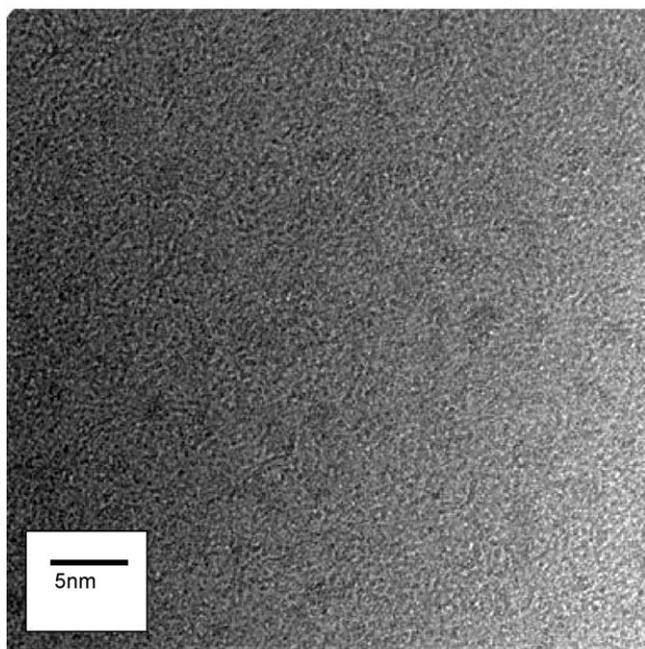
Fig. 6. Micrography and histogram for silica supported niobium oxide nanoparticles, $Nb_2O_5/SiO_2$, obtained from the reduction of $NbCl_4 \cdot 2THF$ with $K[BEt_3H]$.

activity results for silica supported titanium oxide nanoparticles. When the reaction with TBHP took place under an argon atmosphere during 24 h, the conversion goes down to 1.7% (TN: 7.4) for cyclohexene. This result leads to two possible explanations:

(a) that dioxygen is involved in the reaction and TBHP is acting as the initiator of the catalysis; (b) there could be two parallel reactions taking place, one with molecular oxygen and one with TBHP.

When the cyclohexene oxidation reaction takes place only in the presence of oxygen, without TBHP in the reaction mixture, no activity is observed. This indicates that, apparently, the TBHP is acting as an initiator.

In another experiment, the oxidation of cyclohexene was carried out using $H_2O_2$ as the oxidizing agent in the presence of molecular oxygen with methanol as the solvent at 150 °C during 24 h. In this case, the conversion observed was only 3.4% (TN: 17.5).

As can be seen in Table 1, the efficiencies obtained for TBHP are greater than 100%, even though this is the limiting agent, again this corroborates that this oxidizing agent is acting as a catalysis initiator. The TBHP efficiencies were determined assuming that one mol of TBHP consumed produces 1 mol of oxygenated products. The amount of TBHP consumed was determined through iodometric analysis [20].

The reactivity of the silica supported titanium oxide nanoparticles towards the oxo-functionalization of cyclohexane generated 20% conversion (TN: 144) with a 100% selectivity towards the oxidation products after 24 h. For this case, the TBHP efficiency was 471 with respect to the oxidation products. At the beginning of the reaction, the cyclohexanol/cyclohexanone ratio was 1.2, and after 24 h, there is a slight increase in the ratio to 1.4. This result indicates that there is very little over oxidation of the cyclohexanol.

The titanium content determined after the reaction indicates around 8% lixiviation of the metal from the nanostructured material.

Vanadium oxide nanoparticles show high activity towards the oxidation of 1-hexene, cyclohexene and cyclohexane, obtaining turnover of 1190, 878 and 562, respectively (TN: mol of product/mol of vanadium) after 6 h of reaction time (Table 2 and Fig. 8). These correspond to 89.3%, 53.4% and 37.4% conversions for 1-hexene, cyclohexene, cyclohexane, respectively. As can be seen from the comparison data from Tables 1 and 2, the vanadium-based catalyst is at least four-fold more active towards oxidation products than the titanium-based catalyst. It is important to point out that the vanadium oxide catalyst is less selective towards epoxide formation in the case of 1-hexene and

Table 1

Conversion of the catalytic oxidation of 1-hexene, cyclohexene and cyclohexane using $TiO_2/SiO_2$ catalyst[a]

| Catalyst | % Metal | Size (nm) | Substrate | Oxidation agent | TN[b] (% conversion) | | | | % Efficiency TBHP[c] |
|---|---|---|---|---|---|---|---|---|---|
| | | | | | 2 h | 4 h | 6 h | 24 h | |
| $TiO_2/SiO_2$ | 1.8 | 1.9 | 1-Hexene | TBHP | 220 (51.7) | 288 (67.7) | 321.6 (77.5) | 312 (76) | 825 |
| | | | Cyclohexene | TBHP | 174 (33.8) | 274.6 (50.5) | 309.6 (68.4) | 319.6 (76.7) | 507 |
| | | | | $H_2O_2$[d] | – | – | – | 17,5 (3.4) | – |
| | | | Cyclohexane[c] | TBHP | 32 (6.31) | 85 (14) | 133 (19.2) | 144 (20) | 471 |

Molar ratio substrate:TBHP:metal = 500:50:1.

[a] Reaction conditions: 100 mg of catalyst, 0.5 ml of TBHP, 2 ml of the substrate, 1 atm molecular oxygen.

[b] TN: mol of product/mol of titanium.

[c] % Efficiency after 24 h reaction time: (mol of oxidation product/mol of TBHP consumed) × 100.
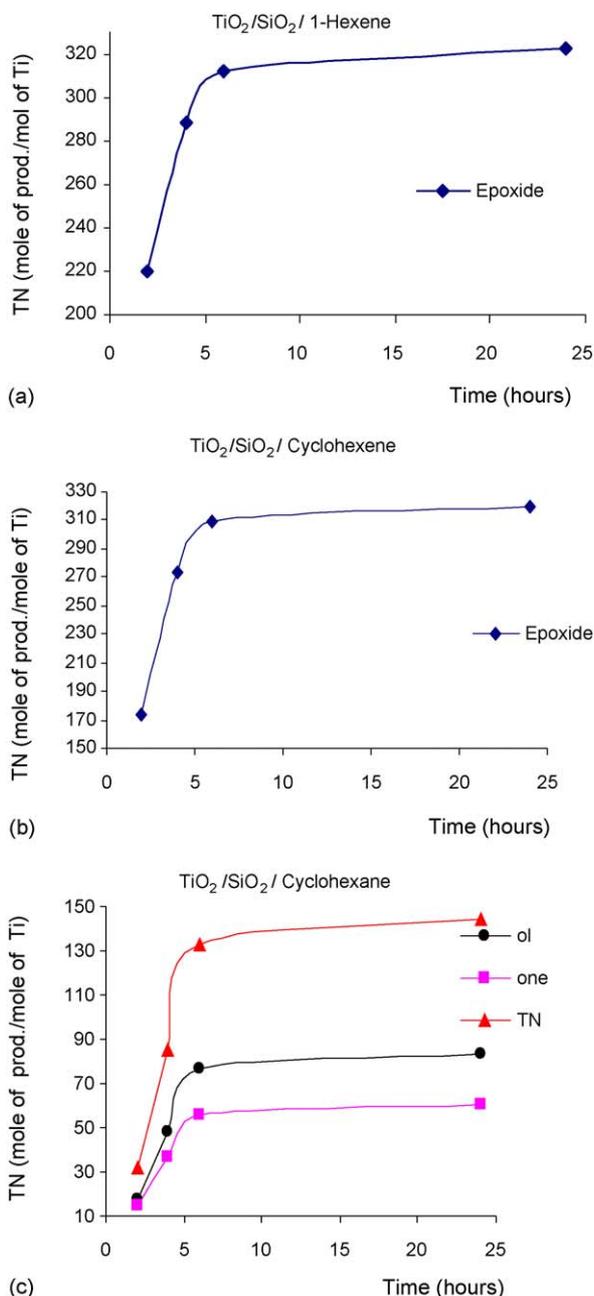
[d] Methanol was used as solvent.

Fig. 7. Catalytic activity and selectivity of nanostructured TiO$_2$/SiO$_2$ catalyst as a function of time, in the oxidation of: (a) 1-hexene, (b) cyclohexene and (c) cyclohexane, with TBHP as the oxidizing agent, 80 °C, molecular oxygen at 3 atm.



Fig. 8. Catalytic activity and selectivity of nanostructured V$_2$O$_5$/SiO$_2$ catalyst as a function of time, in the oxidation of: (a) 1-hexene, (b) cyclohexene and (c) cyclohexane, with TBHP as oxidizing agent, 80 °C, 3 atm molecular oxygen.

very different oxidation products are obtained for the reaction with cyclohexene (2-cyclohexen-1-ol and 2-cyclohexen-1-one). The vanadium-based catalyst shows 89% selectivity towards oxidation products for the case of 1-hexene; this selectivity is distributed as follows: 76.5% butyloxirene, 10.2% as a mixture of 1-hexen-3-ol and 2-hexen-1-ol and 2.0% hexanal as the main oxidation products (Fig. 8a and Table 3). Additionally, the GC–MS analysis also gives a series of other oxidation products formed to a lesser extent. When cyclohexene is used as substrate (Fig. 8b) there is a 95% selectivity towards the oxidation products. In this reaction, the main products are 2-cyclohexen-1-ol (55.2%) and 2-cyclohexen-1-one (44.8%), which represents an
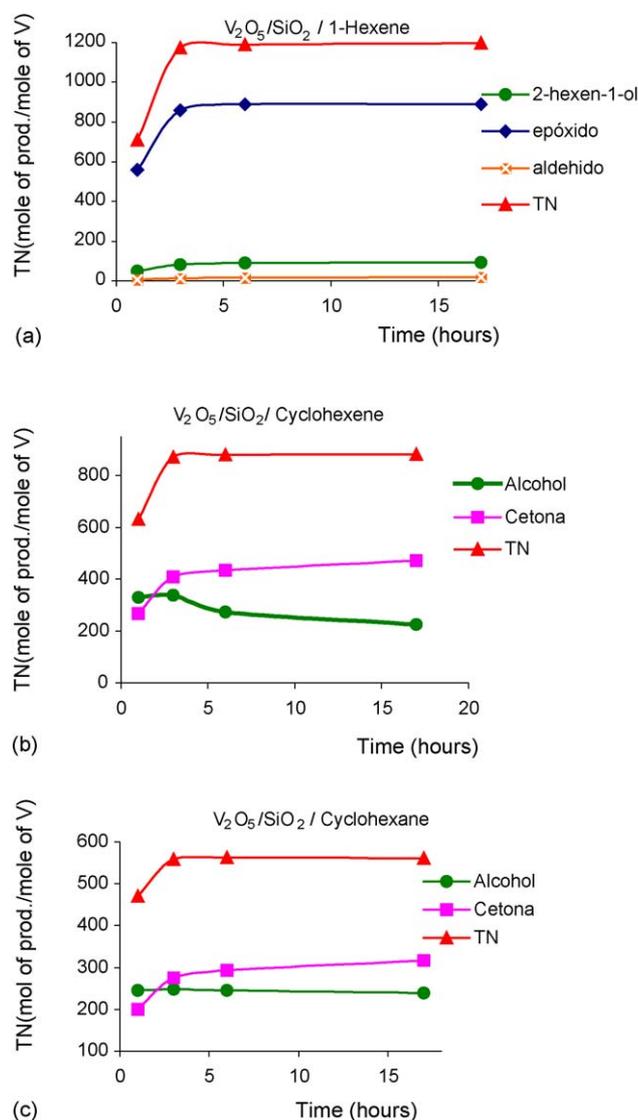
ol/one ratio of 1.2. It is interesting to note that this selectivity is only obtained at the beginning of the reaction, after 3 h the ratio ol/one starts to diminish and at 6 h it has gone down to 0.62. This leads to the belief that there is an over oxidation of the alcohol during the reaction. Fig. 8b shows that for the case of cyclohexene a larger proportion of the oxidation products correspond to the ketone. For the cyclohexane (Fig. 8c) the alcohol and ketone are obtained in almost the same proportions, only a slight over oxidation of the alcohol is observed. The decreasing order of activity for the three substrates are as expected: 1-hexene > cyclohexene > cyclohexane.

When the reaction takes place under molecular oxygen atmosphere but in the absence of TBHP, the vanadium-based catalyst behaves in the same way as the titanium-based catalyst, showing a very low conversion (7.2%). The chemical analysis performed on the catalyst after it had been used in the reaction, reveals a 50% lixiviation of the vanadium metal to the solution. With this result, it is impossible to verify whether the catalysis takes

Table 2
Conversion of the catalytic oxidation of 1-hexene, cyclohexene and cyclohexane using $V_2O_5/SiO_2$ and $Nb_2O_5/SiO_2$ catalysts[a]

| Catalyst | % Metal | Size (nm) | Substrate | Oxidizing agent | TN[b] (% conversion) | | | | % Efficiency TBHP[c] |
|---|---|---|---|---|---|---|---|---|---|
| | | | | | 1 h | 3 h | 6 h | 17 h | |
| $V_2O_5/SiO_2$ | 0.62 | 2.3 | 1-Hexene | TBHP | 810 (60.8) | 1173 (88) | 1190 (89.3) | 1198 (89.8) | 4808 |
| | | | Cyclohexene | TBHP | 630 (33.1) | 870 (52.9) | 878 (53.4) | 882 (53.7) | 3539 |
| | | | Cyclohexane | TBHP | 470 (31.3) | 558 (37.1) | 562 (37.4) | 561 (37.4) | 2337 |
| $Nb_2O_5/SiO_2$ | 0.92 | 1.5 | 1-Hexene | TBHP | 310 (19.3) | 345 (21.6) | 350 (21.8) | 350.6 (31.8) | 210 |
| | | | Cyclohexene | TBHP | 256 (13) | 264.6 (13.4) | 266.6 (13.5) | 267 (13.5) | 182 |
| | | | Cyclohexane | TBHP | 29 (1.6) | 36 (2) | 36.6 (2) | 36.6 (2) | 126.5 |

Molar ratio substrate:TBHP:metal = 1500:150:1.
[a] Reaction conditions: 100 mg of catalyst, 0.5 ml of TBHP, 2 ml of the substrate, 3 atm of molecular oxygen.
[b] TN: mol of product/mol of metal.
[c] % Efficiency after 17 h reaction time: (mol of oxidation product/mol of TBHP consumed) × 100.

place in the heterogeneous system $V_2O_5/SiO_2$, or a mixture of heterogeneous and homogeneous catalysis or whether is it just a homogeneous catalysis taking place.

For the niobium oxide nanoparticles supported on silica, the results reveal that this solid is capable of oxidizing the three substrates used in this study. After 6 h of reaction, the turnovers are 350.0, 266.4 and 36.5; these correspond to 21.8%, 13.5% and 2.0% conversions for 1-hexene, cyclohexene and cyclohexane, respectively (Table 2). Fig. 9 shows the turnover results towards oxidation products with the different substrates studied. For the case of 1-hexene 96%, selectivity towards the oxidation products is found, 1-hexen-3-ol (48.6%) and 2-hexen-1-ol (51.4%) is obtained. Additionally, the GC–MS analysis showed the presence of other oxidation products that are formed to a lesser extent. These results shows that, for 1-hexene, the niobium oxide nanoparticles supported on silica are less active than their titanium and vanadium counterparts under the conditions studied; nevertheless, in this particular case the niobium oxide particles show a different selectivity, where the oxidation products are only alcohols. When the cyclohexene is used as substrate, 97.6% selectivity towards the oxidation products is obtained at the beginning of the reaction, 2-cyclohexen-1-

ol (60%) and 2-cyclohexen-1-one (40%) (Fig. 9b). The ol/one ratio after 1-h reaction time is 1.5, but this ratio starts to diminish after 3 h and at 17 h, it has fallen as far as 0.87. Again, an over oxidation of the alcohol seems evident in this case.

For the cyclohexane (Fig. 9c) 99.5% selectivity towards the oxidation products is obtained, 98% cyclohexanol and 2% cyclohexanone are produced in this reaction.

Once again, it is observed that at the beginning of the reaction there is a high ol/one ratio (57:1), which in time starts to diminish in time reaching a ratio as low as 3:1 after 17 h of reaction time. In this case, the predominant oxidation product is the alcohol.

After the reaction, the ICP analysis of niobium-based catalyst did not show lixiviation which means that this is a heterogeneous catalytic system.

Table 3 presents a summary of the catalytic activity and selectivity of the $TiO_2$, $V_2O_5$ and $Nb_2O_5$ silica supported nanostructured systems towards the oxidation reactions of 1-hexene, cyclohexene and cyclohexane.

From the literature, it is well established that some transition metal ions can be catalytically activated towards oxidation reactions of certain organic substrates when $H_2O_2$ or $RO_2H$ are used as oxidizing agents [26]. These reactions can be classified in two

Table 3
Summary of the catalytic activity and selectivity of the Ti, V and Nb nanostructured systems towards the oxidation of 1-hexene, cyclohexene and cyclohexane[a]

| Catalyst (% metal) | Substrate | TOF (mol of product/mol of metal h) | Selectivity (%) | | | Efficiency TBHP (%) | Conversion (%)[b] |
|---|---|---|---|---|---|---|---|
| | | | Epoxide | Alcohol | Ketone | | |
| $SiO_2$ | 1-Hexene | 3[c] | | | | – | – |
| $TiO_2/SiO_2$ (1.8) | 1-Hexene | 54 | 100 | – | – | 825 | 77.5 |
| | Cyclohexene | 51.5 | 100 | – | – | 507 | 68.4 |
| | Cyclohexane | 22.2 | – | 57.4 | 42.5 | 471 | 19.2 |
| $V_2O_5/SiO_2$ (0.62) | 1-Hexene | 198 | 76.5 | 10.2[d] | 2.0[e] | 4808 | 89.8 |
| | Cyclohexene | 146 | – | 38.5 | 61.5 | 3539 | 53.4 |
| | Cyclohexane | 94 | – | 45.5 | 54.5 | 2337 | 37.4 |
| $Nb_2O_5/SiO_2$ (0.92) | 1-Hexene | 58 | – | 48.6 and 51.4[d] | – | 210 | 21.8 |
| | Cyclohexene | 44.4 | – | 51.4 | 49.6 | 182 | 13.5 |
| | Cyclohexane | 6 | – | 98 | 2 | 126 | 2.0 |

[a] Reaction conditions: 100 mg catalyst, 2 ml substrate, 1 ml TBHP, 80 °C, 6 h reaction time.
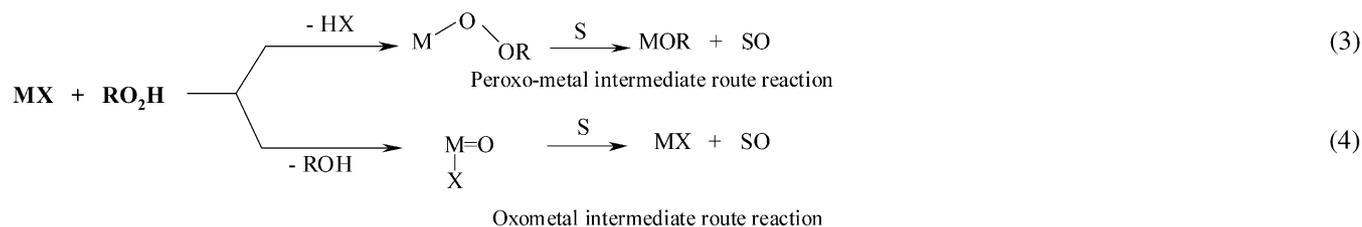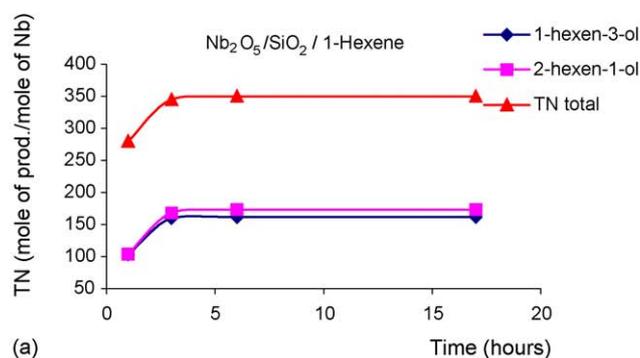[b] After 6 h of reaction time.
[c] TOF: mol product/mol catalyst h.
[d] A mixture of alcohols was obtained (1-hexen-3-ol and 2-hexen-1-ol).
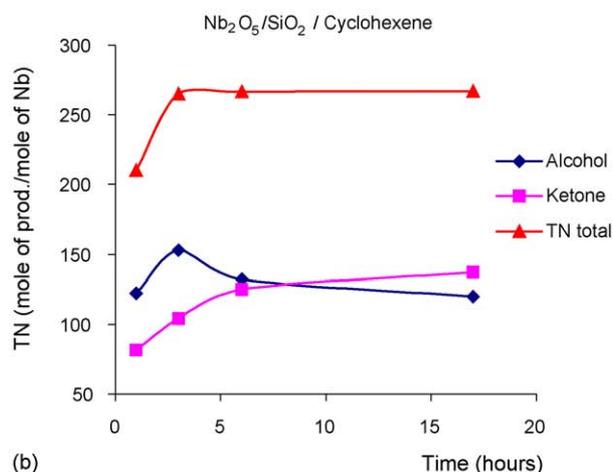[e] Hexanal.

categories depending on whether the active species for the oxidation reaction is: (i) a peroxometal species or (ii) an oxometal species [26] (Eqs. (3) and (4)):
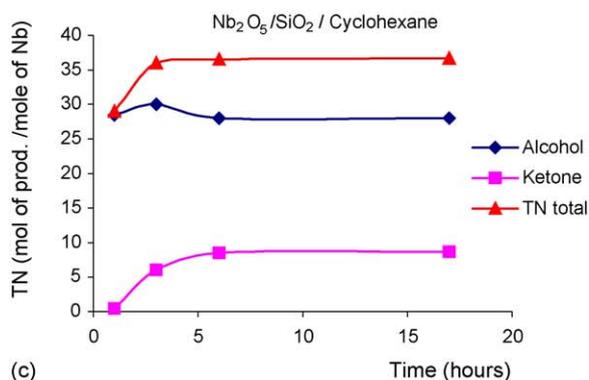
$$\mathbf{MX} + \mathbf{RO_2H} \quad
\begin{cases}
\xrightarrow{\text{- HX}} \quad M\!\!\diagup\!\!\overset{O}{\diagdown}_{OR} \xrightarrow{\;S\;} MOR \;+\; SO \\[2ex]
\xrightarrow{\text{- ROH}} \quad \underset{X}{\overset{}{M}}\!=\!O \xrightarrow{\;S\;} MX \;+\; SO
\end{cases}$$

(3)

Peroxo-metal intermediate route reaction

(4)

Oxometal intermediate route reaction

S = substrate



(a)



(b)



(c)

Fig. 9. Catalytic activity and selectivity of nanostructured Nb$_2$O$_5$/SiO$_2$ catalyst as a function of time, in the oxidation of: (a) 1-hexene, (b) cyclohexene and (c) cyclohexane, with TBHP as the oxidizing agent, 80 °C, 3 atm molecular oxygen.

Generally, the early d$^0$ transition metals (Ti(IV), Zr(IV), V(V), Mo(VI) and W(VI)) react via a peroxometal intermediate; where as the late transition metals elements (Cr(VI), V(V), Mn(V), Ru(VI), Ru(VIII) and Os(VIII)) employ an oxometal intermediate. Some elements such as vanadium, depending on the substrate, can use either route. The majority of the transition metals that catalyse oxygen transfer processes whether via peroxometal or oxometal are also able to catalyse processes via free radicals formed from peroxide compounds [27,28].

Due to the great selectivity shown towards the epoxide formation by the nanostructured TiO$_2$/SiO$_2$ system with 1-hexene and cyclohexene, the free radical mechanism can be discarded. The results obtained with the nanostructured TiO$_2$/SiO$_2$ system encourage us to propose that the primary route is the oxometal intermediate, where the TBHP and the molecular oxygen are both involved to produce the epoxide selectively. Although this type of reaction route has not been proposed for titanium bulk materials, the results presented here indicate that this titanium nanostructured system behaves in this manner.

The selectivity towards the epoxide formation in the oxidation reaction of 1-hexene and cyclohexene obtained in this work for the TiO$_2$/SiO$_2$ nanostructured system, is comparable to that reported by Sensarma et al. [24] for a grafted Ti(O$^i$Pr)$_4$ supported on a preactivated silica. Nevertheless, these authors report higher conversions for the cyclohexene oxidation than for 1-hexene. Also our system shows greater selectivity and activity than the more recently reported by Sreethawong et al. [25] for the catalytic cyclohexene epoxidation by nanocrystalline mesoporous TiO$_2$ (11.1 nm), using as oxidizing agent TBHP generated in situ, in the presence of oxygen from the air.

According to the results obtained for V$_2$O$_5$/SiO$_2$, subsequent studies are under way to determine whether heterogeneous or homogeneous catalysis or both are involved.

The differences observed in the selectivity of V$_2$O$_5$/SiO$_2$ and Nb$_2$O$_5$/SiO$_2$ compared with TiO$_2$/SiO$_2$, could be explained in terms of the Lewis acidity of the metallic centres. It is established in the literature that the acidity of the active centres jointly with the redox properties of the metal determine the selectivity of the catalyst towards oxidation products [29]. For example, the epoxide ring opens on strong Lewis acid sites. This means that if the acid centres are present, the acidic power cannot be too strong when the epoxide product selectivity is aimed [29]. The results reveal (Table 3), that the TiO$_2$/SiO$_2$, V$_2$O$_5$/SiO$_2$, Nb$_2$O$_5$/SiO$_2$ systems seem to have the following relative order of Lewis acidity: TiO$_2$/SiO$_2$ < V$_2$O$_5$/SiO$_2$ < Nb$_2$O$_5$/SiO$_2$.

This Lewis order of acidity is in agreement with other results reported in the literature for bulk mesoporous systems of these metals [29].

From the lixiviation results it is possible to establish that the systems studied within have the following stability order $Nb_2O_5/SiO_2 > TiO_2/SiO_2 > V_2O_5/SiO_2$, once again the behaviour of these nanostructured materials is the same as bulk mesoporous systems of these metals reported in the literature [30].

## 4. Conclusions

Titanium (1.9 nm), vanadium (2.5 nm) and niobium (1.6 nm) oxide nanoparticles stabilized on silica were obtained by the reduction of $TiCl_4 \cdot 2THF$, $VCl_3 \cdot 3THF$ and $NbCl_4 \cdot 2THF$ with $K[BEt_3H]$.

The nanostructured systems reported in this work, $TiO_2/SiO_2$, $V_2O_5/SiO_2$, $Nb_2O_5/SiO_2$, have proved to be active catalysts in the oxidation reactions of 1-hexene, cyclohexene, cyclohexane in the presence of molecular oxygen and TBHP as the oxidizing agent. The $TiO_2/SiO_2$ system is 100% selective towards the production of the epoxide when 1-hexene and cyclohexene are used as substrates. For the cyclohexane, the oxidation gave 100% selectivity towards the formation of cyclohexanol (58%) and cyclohexanone (42%).

The $V_2O_5/SiO_2$ predominantly produced the epoxide for the 1-hexene with high selectivity, nevertheless, for the oxidation reaction of the cyclohexene, the epoxide is not observed and instead 100% selectivity towards the alcohol and the ketone is obtained.

The $Nb_2O_5/SiO_2$ system results gave 100% selective towards alcohols in the case of 1-hexene, but for the cyclohexene substrate, this catalyst shows more or less the same selectivity towards the alcohol and the ketone formation than that found for the vanadium and titanium nanostructured systems. Under the conditions studied, the $Nb_2O_5/SiO_2$ system was less active than the $V_2O_5/SiO_2$ system. It is important to emphasize that the $Nb_2O_5/SiO_2$ system has 98% selectivity towards the alcohol formation for the oxidation of cyclohexane; this behaviour is unique to this particular system. Although as expected, in the oxidation reaction of the cyclohexane, the activity order was $V_2O_5/SiO_2 > TiO_2/SiO_2 > Nb_2O_5/SiO_2$.

It is worth noting that the TBHP efficiency was more than 100% in the oxidation reactions undertaken within the experimental conditions used. Additionally, in this work it was established that molecular oxygen is involved as an oxidizing agent and the TBHP acts as an initiator agent for this catalysis.

## References

[1] R.A. Sheldon, in: R. Ugo (Ed.), Aspects of Homogeneous Catalysis, vol. 4, D. Reidel, Dordrecht, 1981, p. 3.
[2] (a) R.A. Sheldon, J. Mol. Catal. 7 (1980) 107;
    (b) K.A. Jørgensen, Chem. Rev. 89 (1989) 431.
[3] M. Dusi, T. Mallat, A. Baiker, Catal. Rev.: Sci. Eng. 42 (1/2) (2000) 213.
[4] (a) R.A. Sheldon, J.K. Kochi, Metal Catalyzed Oxidation of Organic Compounds, Academic Press, New York, 1981 (Chapter 11);
    (b) U. Schuchardt, D. Cardoso, R. Sercheli, R. Pereira, R.S. Da Cruz, M.C. Guerreiro, D. Mandelli, E.V. Spinacé, E.L. Pires, Appl. Catal. A: Gen. 211 (2001) 1.
[5] F. Wattimena, H.P. Wulff, British Patent 1,249,079 (1971) (to Shell).
[6] R.A. Sheldon, in: B. Cornils, W.A. Hermann (Eds.), Applied Homogeneous Catalysis with Organometallic Compounds, vol. 1, VCH, Weinheim, 1996, p. 411.
[7] F. Maspero, U. Romano, European Patent 0,190,609 (1986).
[8] T. Tatsumi, M. Yako, M. Nakamura, Y. Yahura, H. Tominaga, J. Mol. Catal. A 78 (1993) L41.
[9] J.S. Reddy, A. Sayari, J. Chem. Soc., Chem. Commun. 23 (1995).
[10] (a) H. Arzoumanian, G. Agrifoglio, H. Krentzien, M. Capparelli, New J. Chem. 20 (1996) 699;
    (b) H. Arzoumanian, R. Bakhtchadjian, G. Agrifoglio, H. Krentzien, J.-C. Daran, Eur. J. Inorg. Chem. (1999) 2255.
[11] S. Klein, S. Thorimbert, W.F. Maier, J. Catal. 163 (1996) 476.
[12] R.J. Davis, Z. Liu, Chem. Mater. 9 (1997) 2311.
[13] H. Kochkar, F. Figueras, J. Catal. 171 (1997) 420.
[14] N. Perkas, Y. Koltypin, O. Palchik, A. Gedaken, S. Chandrasekaran, Appl. Catal. A: Gen. 209 (2001) 125.
[15] G. Schmid (Ed.), Clusters and Colloids—From Theory to Applications, VCH, Weinheim, Germany, 1994 (Chapter 6).
[16] C. Burda, X. Chen, R. Narayanan, M.A. El-Sayed, Chem. Rev. 105 (2005) 1025.
[17] L.N. Lewis, Chem. Rev. 93 (1993) 2693.
[18] D.F. Shriver, The Manipulations of Air-Sensitive Compounds, McGraw-Hill, New York, 1969.
[19] H. Bönnemann, G. Braun, W. Brijoux, R. Brikmann, A. Schulze, K. Seevogel, K. Siepen, J. Organometall. Chem. 520 (1996) 143.
[20] I.M. Kolthoff, E.B. Sandel, E.J. Mechan, S. Bruckenstein, Análisis Químico Cuantitativo, 5ta ed., 1979, p. 883.
[21] http://www.lasurface.com and reference within.
[22] E. Jorda, A. Tuel, R. Teissier, J. Kervennal, J. Catal. 175 (1998) 93.
[23] M. Ziolek, I. Nowak, Catal. Today 78 (2003) 543.
[24] S. Sensarma, B.A. Omar, S.L. Scout, H. Alper, J. Mol. Catal. A: Chem. 203 (2003) 145.
[25] T. Sreethawong, Y. Yamada, T. Kobayashi, S. Yoshikawa, J. Mol. Catal. A: Chem. 241 (2005) 23.
[26] I.W.C.E. Arends, R.A. Sheldon, Appl. Catal. A: Gen. 212 (2001) 175.
[27] J.M. Fraile, J.I. García, J.A. Mayoral, E. Vispe, J. Catal. 204 (2001) 146.
[28] G. Busca, E. Finocchio, G. Ramis, G. Ricchiardi, Catal. Today 32 (1996) 133.
[29] M. Ziolek, Catal. Today 78 (2003) 47.
[30] I. Nowak, B. Kilos, M. Ziolek, A. Lewandowska, Catal. Today 78 (2003) 487.